Bioorganic Chemistry 84 (2019) 355–362

Contents lists available at ScienceDirect

Bioorganic Chemistry

journal homepage: www.elsevier.com/locate/bioorg

Combined molecular modeling and cholinesterase inhibition studies on some natural and semisynthetic *O*-alkylcoumarin derivatives

Ilkay Erdogan Orhan[a,*], F. Sezer Senol Deniz[a], Ramin Ekhteiari Salmas[b], Serdar Durdagi[b], Francesco Epifano[c,*], Salvatore Genovese[c], Serena Fiorito[c]

[a] Department of Pharmacognosy, Faculty of Pharmacy, Gazi University, 06330 Ankara, Turkey
[b] Computational Biology and Molecular Simulations Laboratory, Department of Biophysics, School of Medicine, Bahcesehir University, 34349 Istanbul, Turkey
[c] Dipartimento di Farmacia, Università "G. d'Annunzio" Chieti-Pescara, Via dei Vestini 31, 66100 Chieti Scalo, CH, Italy

ARTICLE INFO

Keywords:
Coumarins
Cholinesterase
Butyrylcholinesterase
Enzyme inhibition
Molecular docking
Pharmacokinetic analysis

ABSTRACT

Coumarins of synthetic or natural origins are an important chemical class exerting diverse pharmacological activities. In the present study, 26 novel O-alkylcoumarin derivatives were synthesized and have been tested at 100 μM for their *in vitro* inhibitory potential against acetylcholinesterase (AChE) and butyrlcholinesterase (BChE) targets which are the key enzymes playing role in the pathogenesis of Alzheimer's disease. Among the tested coumarins, none of them could inhibit AChE, whereas 12 of them exerted a marked and selective inhibition against BChE as compared to the reference (galanthamine, IC_{50} = 46.58 ± 0.91 μM). In fact, 10 of the active coumarins showed higher inhibition (IC_{50} = 7.01 ± 0.28 μM – 43.31 ± 3.63 μM) than that of galanthamine. The most active ones were revealed to be 7-styryloxycoumarin (IC_{50} = 7.01 ± 0.28 μM) and 7-isopentenyloxy-4-methylcoumarin (IC_{50} = 8.18 ± 0.74 μM). In addition to the *in vitro* tests, MetaCore/MetaDrug binary QSAR models and docking simulations were applied to evaluate the active compounds by ligand-based and target-driven approaches. The predicted pharmacokinetic profiles of the compounds suggested that the compounds reveal lipophilic character and permeate blood brain barrier (BBB) and the ADME models predict higher human serum protein binding percentages (> 50%) for the compounds. The calculated docking scores indicated that the coumarins showing remarkable BChE inhibition possessed favorable free binding energies in interacting with the ligand-binding domain of the target. Therefore, our results disclose that O-alkylcoumarins are promising selective inhibitors of cholinesterase enzymes, particularly BChE in our case, which definitely deserve further studies.

1. Introduction

Coumarins are a class of natural compounds virtually ubiquitous in the plant kingdom and consist of a 1,2-benzopyrone ring system as a basic parent moiety since the discovery of the first coumarin more than 200 years ago [1]. A high number of substituted coumarins of natural and semisynthetic origin have been isolated from plant and fungal sources and/or chemically synthesized. Such products exert a wide range of pharmacological effects, being able to act as anti-diabetic, anti-viral, anti-microbial, anticancer, anti-oxidant, anti-parasitic, anti-helminthic, anti-proliferative, anti-convulsant, anti-inflammatory, and antihypertensive agents [2]. Many of the research interests have been focused on simple coumarins or furano- or pyranocoumarins, either linear or angular, while much less attention has been dedicated to oxyprenylated ones. These are compounds of mixed metabolic origin for which the coumarin core is attached to a simple or substituted 3,3-dimethylallyl, monoterpenyl or sesquiterpenyl chains *via* an ethereal link. These rare secondary metabolites have displayed a promising pattern of pharmacological activities and a great potential [3]. So far, many coumarin derivatives of natural and synthetic origins have been reported to exert a noteworthy cholinesterase (ChE) inhibitory effect, [4–7]. ChE family consisting of acetylcholinesterase (AChE, syn. acetycholine acetylhydrolase, E.C. 3.1.1.7) and butyrylcholinesterase (BChE, syn. pseudocholinesterase, plasma cholinesterase, E.C. 3.1.1.8)

Abbreviations: AChE, acetylcholinesterase; BChE, butyrylcholinesterase; AD, Alzheimer's Disease; QSAR, Quantitative structure–activity relationship; MCC, Matthews Correlation Coefficient; PDB, Protein Data Bank; BBB, blood brain barrier; ADME, "absorption, distribution, metabolism, and excretion"; HAS, human serum albumin; hERG, human ether a-go-go-related gene

* Corresponding authors.
E-mail addresses: iorhan@gazi.edu.tr (I.E. Orhan), fepifano@unich.it (F. Epifano).

https://doi.org/10.1016/j.bioorg.2018.11.044
Received 10 October 2018; Received in revised form 21 November 2018; Accepted 24 November 2018
Available online 26 November 2018
0045-2068/

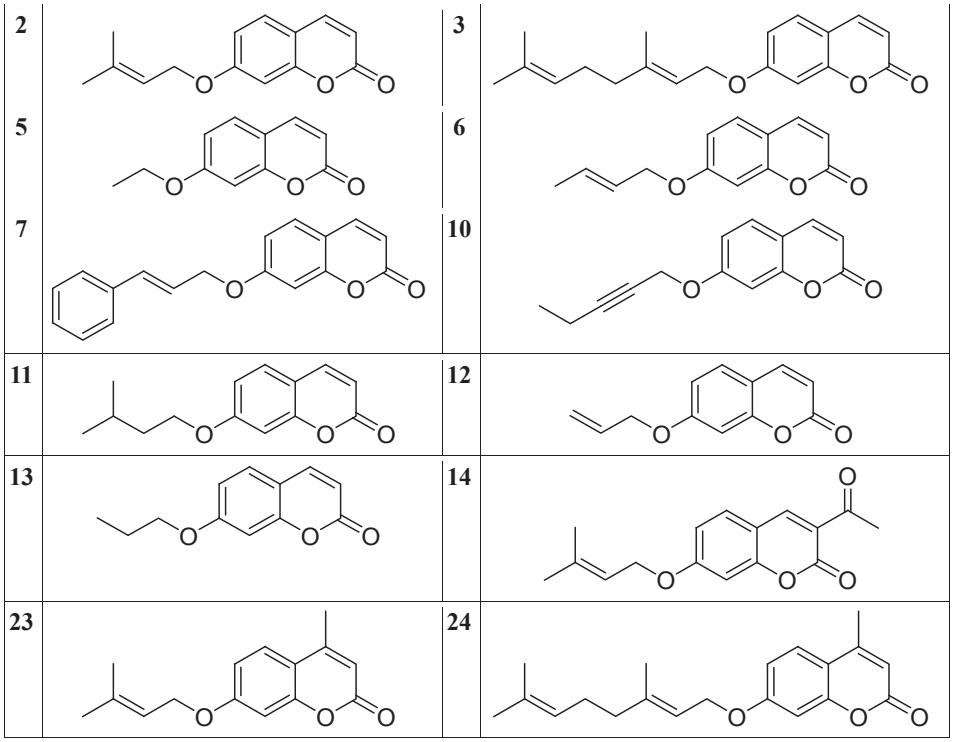

Fig. 1. Chemical structures of the active compounds against BChE.

plays a key role in the pathology of Alzheimer's Disease (AD) and, therefore, ChE inhibitors are used in clinic for the symptomatic treatment of AD since deficiency in acetylcholine/butyrylcholine levels has been shown in the brains of AD patients.

In the context of our ongoing studies to define the phytochemical and biological properties of oxyprenylated secondary metabolites of plant and fungal origin, we wish to report herein the investigation on the interaction of some natural and semisynthetic *O*-alkylcoumarins with promising ChE inhibitory effect by *in vitro* and *in silico* approaches. On this purpose, 26 products (Fig. 1) have been tested *in vitro* against AChE and BChE using high-throughput screening system, while the active inhibitors were proceeded to *in silico* experiments (Tables 2–3, Figs. 2–4). The natural sources of compounds **1–4**, **9**, **11, 14**, **15**, **23** and **24** have been described previously [8]. All other coumarins have been obtained by chemical synthesis. Briefly, the parent hydroxycoumarins were alkylated with the respective alkyl bromide or iodide in acetone and in the presence of dry K_2CO_3 as the base at 80 °C for 1 h (Scheme 1).

2. Materials and methods

2.1. Cholinesterase inhibition

AChE and BChE inhibitory activity of the compounds was measured by slightly modified spectrophotometric method of Ellman [9]. Electric eel AChE (Type-VI-S; EC 3.1.1.7, Sigma, St. Louis, MO, USA) and horse serum BChE (EC 3.1.1.8, Sigma, St. Louis, MO, USA) were used, while acetylthiocholine iodide and butyrylthiocholine chloride (Sigma, St. Louis, MO, USA) were employed as the substrates of these assays, respectively. 5,5′-Dithio-bis(2-nitrobenzoic) acid (DTNB; Sigma, St. Louis, MO, USA) was used for the measurement of the anticholinesterase activity. All reagents and conditions were the same as described in our previous publication [10]. Briefly, in this method, 140 µL of sodium phosphate buffer (pH 8.0), 20 µL of DTNB, 20 µL of test solution and 20 µL of AChE/BChE solution were added by multichannel automatic pipette (Gilson pipetman, Paris, France) in a 96-well microplate and incubated for 15 min at 25 °C. The reaction was then initiated with the

Table 1
Inhibition % ± S.D. and IC_{50} values of the coumarins (1–26) screened against AChE and BChE.

No.	Inhibition% ± S.D.[a] at 100 µM[b]	
	AChE	BChE
1	–[c]	15.18 ± 2.80
2	12.51 ± 2.83	86.92 ± 1.04 (IC_{50} = 11.77 ± 0.89 µM)
3	6.75 ± 2.20	59.18 ± 2.80 (IC_{50} = 12.68 ± 2.23 µM)
4	–	26.66 ± 1.11
5	9.76 ± 1.92	55.98 ± 1.89 (IC_{50} = 83.65 ± 2.39 µM)
6	9.75 ± 2.09	82.25 ± 0.61 (IC_{50} = 16.49 ± 0.99 µM)
7	26.72 ± 1.93	79.69 ± 0.95 (IC_{50} = 7.01 ± 0.28 µM)
8	–	26.77 ± 1.35
9	4.32 ± 1.01	46.53 ± 2.39
10	12.01 ± 1.64	82.50 ± 0.43 (IC_{50} = 18.48 ± 0.73 µM)
11	8.22 ± 0.88	82.66 ± 1.29 (IC_{50} = 23.32 ± 0.57 µM)
12	11.21 ± 2.37	71.72 ± 1.16 (IC_{50} = 43.31 ± 3.63 µM)
13	11.40 ± 1.20	71.89 ± 1.95 (IC_{50} = 39.89 ± 3.90 µM)
14	31.14 ± 2.59	88.62 ± 1.34 (IC_{50} = 11.75 ± 1.81 µM)
15	–	16.29 ± 2.03
16	6.14 ± 2.11	17.36 ± 2.71
17	11.47 ± 1.73	15.56 ± 2.85
18	7.03 ± 2.08	16.64 ± 2.64
19	17.23 ± 2.08	23.77 ± 2.19
20	40.39 ± 3.81	–
21	11.70 ± 3.99	7.01 ± 2.73
22	21.33 ± 0.55	21.35 ± 1.53
23	14.92 ± 0.60	91.30 ± 0.82 (IC_{50} = 8.18 ± 0.74 µM)
24	–	51.04 ± 1.88 (IC_{50} = 106.60 ± 3.54 µM)
25	–	23.82 ± 2.41
26	–	10.45 ± 2.92
Reference[d]	IC_{50} = 2.52 ± 0.15 µM	IC_{50} = 46.58 ± 0.91 µM

[a] Standard deviation.
[b] Final concentration.
[c] No inhibition.
[d] Galanthamine HBr.

Table 2
Pharmacokinetic profiles of studied molecules.

Compounds	BBB, log ratio[a]	G-LogP[b]	Prot-bind, %[c]	Prot-bind, log t[d]	WSol, log mg/L[e]	hERG-inh, pKi[f]	SERT-inh, pKi[g]
2	−0.13	3.51	86.05	−0.30	1.97	−0.08	0.74
3	−0.05	4.24	94.26	−0.17	1.15	−0.06	0.41
5	−0.10	2.50	59.21	−0.53	2.78	−0.43	−0.17
6	−0.02	3.30	79.20	−0.30	1.95	−0.43	−0.20
7	−0.09	4.29	88.27	−0.33	1.53	−0.07	0.51
10	−0.02	3.76	82.59	−0.30	1.79	−0.43	0.29
11	−0.13	3.51	86.05	−0.30	1.97	−0.08	0.74
12	−0.04	3.27	76.74	−0.30	1.95	−0.43	0.35
13	−0.04	3.27	76.74	−0.30	1.95	−0.43	0.35
14	−0.71	3.79	90.95	−0.13	1.86	−0.16	0.86
23	−0.11	4.02	93.23	−0.07	1.62	−0.10	0.76
24	−0.02	4.52	93.99	−0.09	0.81	−0.10	0

[a] Blood brain barrier penetration model. The data is expressed as log values of the ratio of the metabolite concentrations in brain and plasma. Cutoff is -0.3. Larger values indicate that the metabolite is more likely to enter the brain. Reference: Thomson Reuters. Model description: N = 107, R2 = 0.89, RMSE = 0.26.

[b] Lipophilicity, log of compound octanol–water distribution. Cutoffs are −0.4 to 5.6. Values greater than 5.6 correspond to overly hydrophobic compounds. Reference: Syracuse Research, PHYSPROP database. Model description: N = 13474, R2 = 0.95, RMSE = 0.21.

[c] Human serum protein binding, %. Cutoff is 50%. A value of more than 95% is highly bound, less than 50% is a low binding metabolite. Reference: Thummel and Shen, 2001 in Goodman & Gilman's The Pharmacological Basis of Therapeutics. Model description: N = 265, R2 = 0.909, RMSE = 10.11.

[d] Affinity to human serum albumin, log value of the retention time. Cutoff is 0. Positive values correspond to higher protein binding, negative values to lower protein binding. An acceptable level of binding is project dependent. The model is based on retention times of compounds assayed by HPLC using an immobilized HSA column. Values are expressed as log values of the retention time. Reference: Colmenarejo, Alvarez-Pedraglio, et al., 2001 (PMID: 11728183). Model description: N = 95, R2 = 0.904, RMSE = 0.2.

[e] Water solubility at 25??C, log mg/L. Cutoffs are from 2 to 4. An acceptable level of solubility is project dependent. Reference: Syracuse Research, PHYSPROP database. Model description: N = 2871, 2 = 0.91, RMSE = 0.54.

[f] Human hERG (human ether a-go-go-related gene) channel inhibition, pKi (uM). Cutoff is −1.7. The higher the value, the higher the inhibition activity. Lower values are preferable. Reference: Thomson Reuters. Model description: N = 196, R2 = 0.93, RMSE = 0.23.

[g] Human serotonin transporter inhibition, pKi (uM). Cutoff is −1.7. The higher the value, the higher the inhibition activity of the metabolite. Thomson Reuters. Model description: N = 256, R2 = 0.91, RMSE = 0.36.

addition of 10 μL of acetylthiocholine iodide/butyrylthiocholine chloride. Hydrolysis of acetylthiocholine iodide/butyrylthiocholine chloride was monitored by the formation of the yellow 5-thio-2-nitrobenzoate anion as a result of the reaction of DTNB with thiocholines, catalyzed by enzymes at 412 nm utilizing a 96-well microplate reader (VersaMax Molecular Devices, Sunnyvale, CA, USA). The measurements and calculations were evaluated by using Softmax PRO 4.3.2.LS software (Sunnyvale, CA, USA). Percentage of inhibition of AChE/BChE was determined by comparison of reaction rates of the samples relative to blank sample (ethanol in phosphate buffer pH = 8) using the formula *(E-S)/E × 100*, where *E* is the activity of enzyme without test sample and *S* is the activity of enzyme with test sample. The experiments were done in triplicate. Galanthamine (Sigma, St. Louis, MO, USA) was used as the reference drug.

2.2. Chemistry

2.2.1. Chemicals

All starting materials (7-hydroxycoumarin, 3-acetyl-7-hydroxycoumarin, 3-chloro-4-methyl-7-hydroxycoumarin, 6,7-dihydroxycoumarin, 4-methyl-7-hydroxycoumarin, 7-hydroxycoumarin-3-carboxylic acid, 4,7-dihydroxycoumarin), reagents, and solvents have been purchased from Merck Sigma Aldrich (Milan, IT), used without further purification. For purification and structural characterization of adducts the same general procedures as already reported were followed [1]. All synthesized products were obtained with a purity > 96.7% assessed by HPLC.

2.2.2. General procedure for alkylation of 7-hydroxycoumarins

To a solution of 7-hydroxycoumarin (1.0 mmol) in acetone (5 mL), dry K_2CO_3 (1.3 mmol) and alkyl bromide (iodide) (1.05 mmol) were added and the resulting suspension was stirred at 80 °C for 1 h. The warm solution was poured into icy water (50 mL) and the resulting precipitate collected by filtration under vacuum yielding the desired adduct.

7-Isopentenyloxycoumarin 2. White solid. Yield 95%. Analytical data were in full agreement with those previously reported for the same compound [1]. Anal. Calc. for $C_{14}H_{14}O_3$: C 73.03, H 6.13, O 20.85; Found: C 72.98, H 6.16, O 20.81.

Auraptene 3. White solid. Yield 98 %Analytical data were in full agreement with those previously reported for the same compound [1]. Anal. Calc. for $C_{19}H_{22}O_3$: C 76.48, H 7.43, O 16.09; Found: C 76.44, H 7.40, O 16.04.

Umbelliprenin 4. White waxy solid. Yield 88 %Analytical data were in full agreement with those previously reported for the same compound [2]. Anal. Calc. for $C_{24}H_{302}O_3$: C 78.65, H 8.25, O 13.10; Found: C 78.61, H 8.22, O 13.08.

7-Ethoxycoumarin 5. White solid. Yield 99 %Analytical data were in full agreement with those previously reported for the same compound [1]. Anal. Calc. for $C_{11}H_{10}O_3$: C 69.46, H 5.30, O 25.24; Found: C 69.49, H 5.25, O 25.20.

7-(2′-Butenyloxy)coumarin 6. White solid. Yield 90%. Analytical data were in full agreement with those previously reported for the same compound [1]. Anal. Calc. for $C_{13}H_{12}O_3$: C 72.21, H 5.59, O 22.20; Found: C 72.17, H 5.55, O 22.23.

7-Styryloxycoumarin 7. Yellowish solid, m.p. 79–81 °C. Yield 93%. ^{1}H NMR δ 4.64–4.66 (m, 2H), 6.18–6.21 (d, 1H, *J* = 3.4 Hz), 6.39–7.38 (m, 10H), 7.58–7.61 (d, 1H, *J* = 3.4 Hz); ^{13}C NMR δ 69.4, 100.9, 112.4, 112.7, 112.8, 123.8, 127.0, 128.1, 128.8, 129.4, 134.9, 136.2, 143.1, 155.6, 160.8, 162.8. Anal. Calc. for $C_{18}H_{14}O_3$: C 77.68, H 5.07, O 17.25; Found: C 77.63, H 5.09, O 17.29.

7-(2′,2′-Dimethyl)-*n* propoxycoumarin 8. White solid. Yield 88%. Analytical data were in full agreement with those obtained from a commercial sample. Anal. Calc. for $C_{14}H_{16}O_3$: C 72.39, H 6.94, O 20.66; Found: C 72.32, H 6.91, O 20.69.

7-Methoxycoumarin 9. White solid. Yield 99%. Analytical data were in full agreement with those previously reported for the same compound [1]. Anal. Calc. for $C_{10}H_8O_3$: C 68.18, H 4.58, O 27.25; Found: C 68.22, H 4.56, O 27.21.

7-(2′-Pentinyloxy)coumarin 10. Yellowish solid. Yield 84%. Analytical data were in full agreement with those previously reported for the same compound [1]. Anal. Calc. for $C_{14}H_{12}O_3$: C 73.67, H 5.30, O 21.03; Found: C 73.66, H 5.26, O 21.08.

7-(3′-Methyl)-*n*butyloxy)coumarin 11. White solid. Yield 88%. Analytical data were in full agreement with those previously reported for the same compound [1]. Anal. Calc. for $C_{14}H_{16}O_3$: C 72.39, H 6.94, O 20.66; Found: C 72.36, H 6.89, O 20.61.

7-Allyloxycoumarin 12. White solid. Yield 960%. Analytical data were in full agreement with those previously reported for the same compound [1]. Anal. Calc. for $C_{12}H_{10}O_3$: C 71.28, H 4.98, O 23.74; Found: C 71.33, H 4.96, O 23.79.

7-*n*Propoxycoumarin 13. White solid. Yield 99%. Analytical data were in full agreement with those previously reported for the same compound [1]. Anal. Calc. for $C_{12}H_{12}O_3$: C 70.57, H 5.92, O 23.50; Found: C 70.51, H 5.91, O 23.48.

3-Acetyl-7-isopentenyloxycoumarin 14. Yellowish solid. Yield 84%. Analytical data were in full agreement with those previously

Table 3
Prediction of toxicity values of studied molecules.

Toxicity activity	2	3	5	6	7	10	11	12	13	14	23	24
AMES (1)	0.24	0.16	0.16	0.34	0.21	0.34	0.24	0.27	0.27	0.58	0.33	0.15
Anemia (2)	0.34	0.19	0.39	0.42	0.22	0.38	0.34	0.41	0.41	0.27	0.33	0.19
Carcinogenicity (3)	0.36	0.14	0.43	0.40	0.15	0.42	0.36	0.40	0.40	0.44	0.35	0.15
Carcinogenicity Mouse Female (4)	0.34	0.19	0.33	0.33	0.19	0.25	0.34	0.40	0.40	0.21	0.32	0.19
Carcinogenicity Mouse Male (5)	0.29	0.16	0.24	0.28	0.31	0.26	0.29	0.31	0.31	0.24	0.27	0.13
Carcinogenicity Rat Female (6)	0.24	0.07	0.29	0.28	0.10	0.17	0.24	0.29	0.29	0.09	0.21	0.07
Carcinogenicity Rat Male (7)	0.58	0.24	0.45	0.52	0.22	0.45	0.58	0.59	0.59	0.38	0.55	0.18
Cardiotoxicity (8)	0.58	0.57	0.45	0.45	0.55	0.44	0.58	0.45	0.45	0.67	0.55	0.55
Cytotoxicity model, -log GI50 (M) (9)	4.86	5.19	4.80	4.84	4.82	4.61	4.86	4.84	4.84	4.95	4.86	5.05
Epididymis toxicity (10)	0.85	0.83	0.83	0.85	0.84	0.83	0.85	0.85	0.85	0.73	0.85	0.83
Genotoxicity (11)	0.24	0.26	0.23	0.27	0.43	0.29	0.24	0.25	0.25	0.19	0.19	0.19
Hepatotoxicity (12)	0.60	0.56	0.76	0.62	0.43	0.69	0.60	0.66	0.66	0.58	0.60	0.53
Kidney Necrosis (13)	0.28	0.17	0.54	0.52	0.39	0.47	0.28	0.60	0.60	0.27	0.26	0.17
Kidney Weight Gain (14)	0.63	0.49	0.91	0.90	0.40	0.88	0.63	0.91	0.91	0.59	0.63	0.49
Liver Cholestasis (15)	0.70	0.70	0.68	0.70	0.68	0.70	0.70	0.70	0.70	0.70	0.70	0.70
Liver Lipid Accumulation (16)	0.54	0.48	0.40	0.57	0.49	0.59	0.54	0.50	0.50	0.53	0.55	0.50
Liver Necrosis (17)	0.25	0.39	0.50	0.66	0.92	0.62	0.25	0.68	0.68	0.37	0.24	0.28
Liver Weight Gain (18)	0.32	0.29	0.44	0.78	0.89	0.81	0.32	0.80	0.80	0.38	0.40	0.29
MRTD (19)	0.42	0.39	0.55	0.40	0.45	0.40	0.42	0.40	0.40	0.29	0.35	0.33
Nasal pathology (20)	0.21	0.13	0.28	0.11	0.22	0.11	0.21	0.13	0.13	0.05	0.12	0.12
Nephron Injury (21)	0.53	0.57	0.70	0.71	0.75	0.72	0.53	0.66	0.66	0.26	0.33	0.32
Nephrotoxicity (22)	0.50	0.50	0.80	0.65	0.41	0.65	0.50	0.68	0.68	0.41	0.49	0.47
Neurotoxicity (23)	0.77	0.51	0.78	0.75	0.71	0.68	0.77	0.78	0.78	0.68	0.73	0.49
Pulmonary toxicity (24)	0.56	0.60	0.76	0.47	0.56	0.52	0.56	0.50	0.50	0.34	0.62	0.64
SkinSens, EC3 (25)	17.63	19.67	11.95	12.25	12.19	10.44	17.63	15.87	15.87	22.42	22.96	22.55
Testicular toxicity (26)	0.40	0.41	0.41	0.46	0.44	0.48	0.40	0.45	0.45	0.34	0.42	0.43

1. Potential to be mutagenic (AMES positive), range from 0 to 1. A value of 1 is AMES positive (mutagenic), and a value of 0 is AMES negative (non-mutagenic). Cutoff is 0.5. Values close to zero are preferable. The AMES assay is based upon the reversion of mutations in the histidine operon in the bacterium Salmonella enterica sv Typhimurium.

2. Potential for causing anemia. Cutoff is 0.5. Values higher than 0.5 indicate potentially toxic compounds. Training set consists of chemicals and drugs causing anemia in vivo. Model organisms: human. Model description: Training set N = 324, Test set N = 51, Sensitivity = 0.82, Specificity = 0.90, Accuracy = 0.86, MCC = 0.72.

3. Potential for inducing carcinogenicity in rats and mice. Cutoff is 0.5. Values higher than 0.5 indicate potentially toxic.
compounds. Training set consists of chemicals and drugs causing carcinogenicity in vivo. Model organisms: mouse, rat. Model description: Training set N = 1210, Test set N = 185, Sensitivity = 0.96, Specificity = 0.90, Accuracy = 0.93, MCC = 0.86.

4. Potential for inducing carcinogenicity in female mice. Cutoff is 0.5. Values higher than 0.5 indicate potentially toxic compounds. Training set consists of chemicals and drugs causing carcinogenicity in vivo. Model organisms: female mice. Model description: Training set N = 640, Test set N = 94, Sensitivity = 0.90, Specificity = 0.93, Accuracy = 0.92, MCC = 0.83.

5. Potential for inducing carcinogenicity in male mice. Cutoff is 0.5. Values higher than 0.5 indicate potentially toxic compounds. Training set consists of chemicals and drugs causing carcinogenicity in vivo. Model organisms: mouse male. Model description: Training set N = 584, Test set N = 93, Sensitivity = 0.91, Specificity = 0.88, Accuracy = 0.89, MCC = 0.78.

6. Potential for inducing carcinogenicity in female rats. Cutoff is 0.5. Values higher than 0.5 indicate potentially toxic compounds. Training set consists of chemicals and drugs causing carcinogenicity in vivo. Model organisms: female rat. Model description: Training set N = 667, Test set N = 120, Sensitivity = 0.90, Specificity = 0.96, Accuracy = 0.93, MCC = 0.86.

7. Potential for inducing carcinogenicity in male rats. Cutoff is 0.5. Values higher than 0.5 indicate potentially toxic compounds. Training set consists of chemicals and drugs causing carcinogenicity in vivo. Model organisms: male rat. Model description: Training set N = 715, Test set N = 117, Sensitivity = 0.92, Specificity = 0.88, Accuracy = 0.90, MCC = 0.79.

8. Potential for inducing cardiotoxicity. Cutoff is 0.5. Values higher than 0.5 indicate potentially toxic compounds. Training set consists of chemicals and drugs causing cardiotoxicity in vivo. Model organisms: mouse, rat, human. Model description:Training set N = 143, Test set N = 30, Sensitivity = 0.80, Specificity = 1.00, Accuracy = 0.90, MCC = 0.82.

9. Growth inhibition of MCF7 cell line (human caucasian breast adenocarcinoma), pGI50. Cutoff is 6. Values from 6 to 8 correspond to a toxic metabolite, values less than 6 are preferable, values less than 3 are more preferable and less toxic. Model description: N = 1474, R2 = 0.9, RMSE = 0.05.

10. Potential for inducing epididymis toxicity. Training set consists of chemicals and drugs causing epididymis toxicity in vivo. Model organisms: mouse, rat, human. Cutoff is 0.5. Values higher than 0.5 indicate potentially toxic compounds. Model description: Training set N = 252, Test set N = 42, Sensitivity = 0.90, Specificity = 0.86, Accuracy = 0.88, MCC = 0.76.

11. Potential for inducing genotoxicity. Cutoff is 0.5. Values higher than 0.5 indicate potentially toxic compounds. Training set consists of chemicals and drugs causing genotoxicity in vivo. Model organisms: mouse, rat. Model description: Training set N = 372, Test set N = 86, Sensitivity = 0.75, Specificity = 0.84, Accuracy = 0.79, MCC = 0.59.

12. Potential for inducing hepatotoxicity. Cutoff is 0.5. Values higher than 0.5 indicate potentially toxic compounds. Training set consists of chemicals and drugs causing hepatotoxicity in vivo. Model organisms: mouse, rat, human. Model description: Training set N = 1380, Test set N = 231, Sensitivity = 0.73, Specificity = 0.88, Accuracy = 0.81, MCC = 0.62.

13. Potential for inducing kidney necrosis. Cutoff is 0.5. Values higher than 0.5 indicate potentially toxic compounds. Training set consists of chemicals and drugs causing renal necrosis in vivo. Model organisms: mouse, rat, human. Model description: Training set N = 221, Test set N = 42, Sensitivity = 0.96, Specificity = 1.00, Accuracy = 0.98, MCC = 0.95.

14. Potential for inducing kidney weight gain. Cutoff is 0.5. The values higher than 0.5 indicate potentially toxic compounds. Training set consists of chemicals and drugs causing kidney weight gain in vivo. Model organisms: mouse, rat. Model description: Training set N = 240, Test set N = 49, Sensitivity = 0.95, Specificity = 1.00, Accuracy = 0.98, MCC = 0.96.

15. Potential for inducing liver cholestasis. Cutoff is 0.5. Values higher than 0.5 indicate potentially toxic compounds. Training set consists of chemicals and drugs causing cholestasis in vivo. Model organisms: mouse, rat, human. Model description: Training set N = 218, Test set N = 35, Sensitivity = 0.79, Specificity = 0.67, Accuracy = 0.74, MCC = 0.46.
16. Potential for inducing liver lipid accumulation. Cutoff is 0.5. Values higher than 0.5 indicate potentially toxic compounds. Training set consists of chemicals and drugs causing lipid accumulation in vivo. Model organisms: mouse, rat, human. Model description: Training set N = 172, Test set N = 28, Sensitivity = 0.80, Specificity = 0.85, Accuracy = 0.82, MCC = 0.64.
17. Potential for inducing liver necrosis. Cutoff is 0.5. Values higher than 0.5 indicate potentially toxic compounds. Training set consists of chemicals and drugs causing hepatic necrosis in vivo. Model organisms: mouse, rat, human. Model description: Training set N = 300, Test set N = 57, Sensitivity = 0.91, Specificity = 0.91, Accuracy = 0.91, MCC = 0.82.
18. Potential for inducing liver weight gain. Cutoff is 0.5. Values higher than 0.5 indicate potential liver weight-changing compounds. Training set consists of chemicals and drugs causing liver weight gain in vivo. Model organisms: mouse, rat. Model description: Training set N = 292, Test set N = 52, Sensitivity = 1.00, Specificity = 1.00, Accuracy = 1.00, MCC = 1.00.
19. Maximum Recommended Therapeutic Dose, log mg/kg-bm/day, range is from -5 to 3. Cutoff is 0.5. Chemicals with high log MRTDs can be classified as mildly toxic compounds, chemicals with low log MRTDs as highly toxic compounds. Model description: N = 1209, R2 = 0.86, RMSE = 0.42.
20. Potential for causing nasal pathology. Training set consists of chemicals and drugs causing nasal pathology in vivo. Model organisms: mouse, rat, human. Cutoff is 0.5. Values higher than 0.5 indicate potentially toxic compounds. Model description: Training set N = 246, Test set N = 47, Sensitivity = 1.00, Specificity = 0.93, Accuracy = 0.96, MCC = 0.92.
"chronic neurodegenerative diseases"21. Potential for inducing nephron injury. Cutoff is 0.5. Values higher than 0.5 indicate potentially toxic compounds. Training set consists of chemicals and drugs causing nephron injury in vivo. Model organisms: mouse, rat, human. Model description: Training set N = 598, Test set N = 109, Sensitivity = 0.91, Specificity = 1.00, Accuracy = 0.96, MCC = 0.93.
22. Potential for inducing nephrotoxicity. Cutoff is 0.5. Values higher than 0.5 indicate potentially toxic compounds. Training set consists of chemicals and drugs causing nephrotoxicity in vivo. Model organisms: mouse, rat, human. Model description: Training set N = 847, Test set N = 154, Sensitivity = 0.90, Specificity = 0.84, Accuracy = 0.87, MCC = 0.74.
23. Potential for inducing neurotoxicity. Training set consists of chemicals and drugs causing neurotoxicity in vivo. Model organisms: mouse, rat, human. Cutoff is 0.5. Values higher than 0.5 indicate potentially toxic compounds. Model description: Training set N = 175, Test set N = 34, Sensitivity = 0.94, Specificity = 0.94, Accuracy = 0.94, MCC = 0.88.
24. Potential for inducing pulmonary toxicity. Training set consists of chemicals and drugs causing pulmonary toxicity in vivo. Model organisms: mouse, rat, human. Cutoff is 0.5. Values higher than 0.5 indicate potentially toxic compounds. Model description: Training set N = 482, Test set N = 87, Sensitivity = 0.89, Specificity = 0.88, Accuracy = 0.89, MCC = 0.77.
25. Skin sensitization potential expressed as effective concentration 3, EC3 %. Values higher than 10 indicate weak and moderate sensitizers. Model description: N = 89, R2 = 0.67, RMSE = 22.56.
26. It consists of chemicals and drugs causing testicular toxicity in vivo. Model organisms: mouse, rat, human. Cutoff is 0.5. Values higher than 0.5 indicate potentially toxic compounds. Model description: Training set N = 439, Test set N = 88, Sensitivity = 0.81, Specificity = 0.85, Accuracy = 0.83, MCC = 0.66.

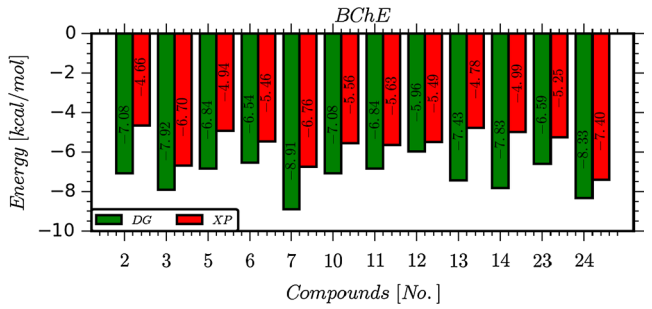

Fig. 2. Top scores of the compounds against to BChE, obtained by GOLD and XP methods are presented as stacked bar plots.

reported for the same compound [3]. Anal. Calc. for $C_{16}H_{16}O_4$: C 70.57, H 5.92, O 23.50; Found: C 70.59, H 5.86, O 23.44.

3-Acetyl-7-geranyloxycoumarin 15. Brownish solid, m.p. 122–124 °C. Yield 83%. ^{1}H NMR δ 1.63 (s, 3H), 1.66 (s, 3H), 1.73 (s, 3H), 2.07–2.12 (m, 4H), 2.54 (s, 3H), 4.37–4.41 (m, 2H), 5.09–5.12 (m, 1H), 5.47–5.50 (m, 1H), 6.82–7.21 (m, 3H), 8.39 (s, 1H); ^{13}C NMR δ 16.7, 17.5, 25.8, 26.2, 31.9, 39.1, 65.2, 101.3, 109.8, 112.8, 119.5, 124.0, 125.1, 130.1, 131.0, 141.5, 146.4, 156.5, 158.2, 161.9, 202.9. Anal. Calc. for $C_{21}H_{24}O_4$: C 74.09, H 7.11, O 18.80; Found: C 74.03, H 7.09, O 18.74.

3-Acetyl-7-farnesyloxycoumarin 16. Brown solid, m.p. 136–138 °C. Yield 78%. ^{1}H NMR δ 1.59 (s, 3H), 1.62 (s, 3H), 1.67 (s, 3H), 1.75 (s, 3H), 2.04–2.18 (m, 8H), 2.60 (s, 3H), 4.56–4.60 (m, 2H), 5.07–5.13 (m, 2H), 5.49–5.52 (m, 1H), 6.84–7.27 (m, 3H), 8.44 (s, 1H); ^{13}C NMR δ 14.8, 16.2, 17.6, 25.6, 26.4, 26.9, 31.9, 39.6, 39.8, 65.2, 101.3, 109.8, 112.8, 119.6, 123.5, 124.7, 125.5, 130.2, 131.0, 135.2, 140.9, 146.0, 156.4, 158.0, 161.7, 202.9. Anal. Calc. for $C_{26}H_{32}O_4$: C 76.44, H 7.90, O 15.67; Found: C 76.39, H 7.91, O 15.61.

3-Chloro-7-isopentenyloxy-4-methylcoumarin 17. White solid, m.p. 126–129 °C. Yield 89%. Analytical data were in full agreement with those previously reported for the same compound [4].

Anal. Calc. for $C_{15}H_{15}ClO_3$: C 64.64, H 7.90, O 15.67; Found: C 64.61, H 7.91, O 15.61.

3-Chloro-7-geranyloxy-4-methylcoumarin 18. Yellowish solid, m.p. 137–139 °C. Yield 85%. ^{1}H NMR δ 1.61 (s, 3H), 1.63 (s, 3H), 1.66 (s, 3H), 2.08–2.12 (m, 4H), 2.55 (s, 3H), 4.38–4.42 (m, 2H), 5.10–5.13 (m, 1H), 5.45–5.48 (m, 1H), 6.31–7.80 (m, 3H); ^{13}C NMR δ 16.3, 17.6, 18.8, 25.6, 26.3, 39.8, 65.1, 102.0, 106.1, 111.2, 112.4, 119.9, 124.0, 126.4, 131.4, 141.6, 144.8, 152.9, 154.9, 162.2. Anal. Calc. for $C_{25}H_{31}ClO_3$: C 72.36, H 7.53, O 11.57; Found: C 72.29, H 7.50, O 11.62.

3-Chloro-7-farenesyloxy-4-methylcoumarin 19. Brownish solid, m.p. 146–149 °C. Yield 73%. ^{1}H NMR δ 1.60, (s, 3H), 1.62 (s, 3H), 1.64 (s, 3H), 1.75 (s, 3H), 2.03–2.11 (m, 8H), 2.54 (s, 3H), 4.55–4.58 (m, 2H), 5.07–5.15 (m, 2H), 5.47–5.51 (m, 1H), 6.35–7.74 (m, 3H); ^{13}C NMR δ 14.9, 16.4, 17.6, 18.9, 25.5, 26.3, 26.6, 39.8, 39.9, 65.1, 101.8, 106.0, 111.0, 112.4, 119.9, 123.5, 124.7, 126.3, 131.0, 135.6, 141.4, 144.8, 152.9, 154.6, 162.2. Anal. Calc. for $C_{30}H_{39}ClO_3$: C 74.59, H 8.14, O 9.94; Found: C 74.52, H 8.15, O 9.91.

6,7-Diisopentenyloxycoumarin 20. White solid, m.p. 101–104 °C. Yield 81%. ^{1}H NMR δ 1.70, (s, 3H), 1.71 (s, 3H), 1.75 (s, 3H), 1.76 (s, 3H), 4.57–4.64 (m, 4H), 5.72–5.79 (m, 2H), 6.28–6.33 (d, 1H, J = 3.7 Hz), 6.74–6.91 (m, 2H), 7.67–7.71 (d, 1H, J = 3.7 Hz); ^{13}C NMR δ 18.9, 27.2, 66.4, 102.9, 109.6, 112.8, 113.9, 119.0, 138.3, 143.1, 143.4, 147.9, 149.8, 160.1. Anal. Calc. for $C_{19}H_{22}O_4$: C 72.59, H 7.05, O 20.36; Found: C 72.53, H 7.02, O 20.33.

6,7-Digeranyloxycoumarin 21. White solid, m.p. 122–125 °C. Yield 72%. ^{1}H NMR δ 1.63 (s, 3H), 1.68 (s, 3H), 1.71, (s, 3H), 1.73 (s, 3H), 1.78 (s, 3H), 1.79 (s, 3H), 2.02–2.11 (m, 8H), 4.68–4.77 (m, 4H), 5.04–5.46 (m, 4H), 6.29–6.32 (d, 1H, J = 3.6 Hz), 6.75–6.91 (m, 2H), 7.65–7.68 (d, 1H, J = 3.6 Hz); ^{13}C NMR δ 16.1, 16.3, 17.6, 17.7, 25.4, 25.6, 26.2, 26.4, 31.6, 39.3, 65.9, 65.9, 102.7, 112.7, 113.5, 119.8, 121.0, 123.9, 124.6, 131.3, 131.8, 136.0, 141.6, 143.0, 143.7, 147.6, 149.9, 160.4. Anal. Calc. for $C_{29}H_{38}O_4$: C 77.30, H 8.50, O 14.20;

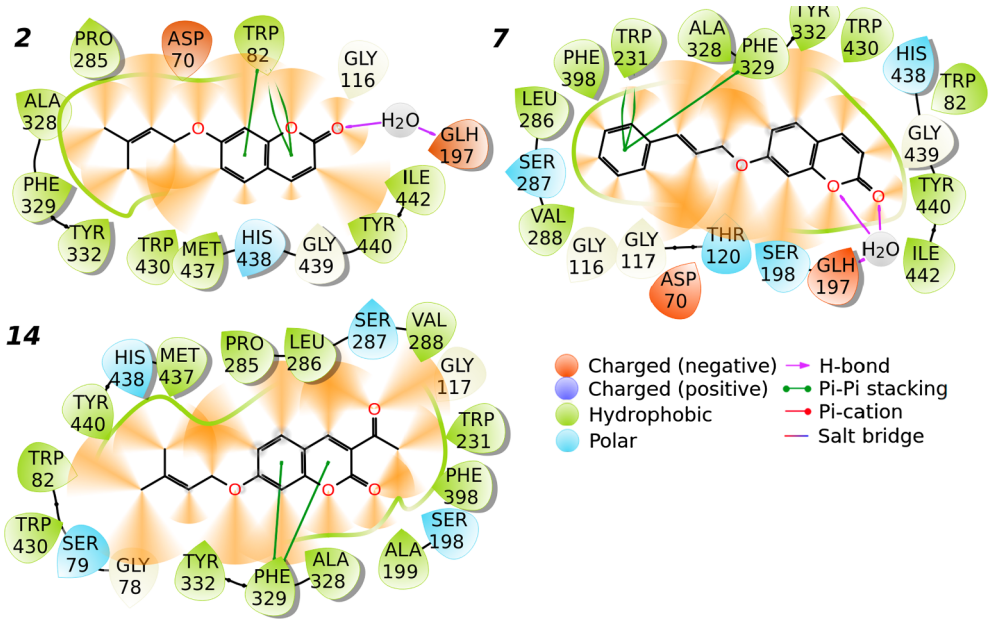

Fig. 3. 2D schematic views of the selected ligands inside the BChE target.

Found: C 77.35, H 8.51, O 14.14.

6,7-Difarnesyloxycoumarin 22. Brownish solid, m.p. 144–147 °C. Yield 71%. ^{1}H NMR δ 1.58 (s 3H), 1.60 (s, 3H), 1.64 (s, 3H), 1.67 (s, 3H), 1.70, (s, 3H), 1.74 (s, 3H), 1.77 (s, 3H), 1.79 (s, 3H), 2.03–2.15 (m, 12H), 4.69–4.79 (m, 4H), 5.07–5.50 (m, 6H), 6.28–6.31 (d, 1H, J = 3.6 Hz), 6.77–6.90 (m, 2H), 7.64–7.67 (d, 1H, J = 3.6 Hz); ^{13}C NMR δ 13.7, 15.0, 16.2, 17.5, 17.6, 17.8, 25.5, 25.7, 26.0, 26.2, 26.5, 26.7, 32.6, 39.5, 39.7, 65.8, 65.9, 102.8, 109.5, 112.8, 113.6, 119.8, 121.9, 123.6, 123.9, 124.4, 124.8, 131.0, 131.2, 135.0, 135.3, 141.7, 143.0, 143.5, 147.6, 150.0, 160.5. Anal. Calc. for $C_{39}H_{54}O_4$: C 79.82, H 9.27, O 10.91; Found: C 79.76, H 9.22, O 10.85.

7-Isopentenyloxy-4-methylcoumarin 23. White solid. Yield 95%. Analytical data were in full agreement with those previously reported for the same compound [8]. Anal. Calc. for $C_{15}H_{16}O_3$: C 73.75, H 6.60, O 19.65; Found: C 73.77, H 6.65, O 19.61.

7-Geranyloxy-4-methylcoumarin 24. White solid. Yield 92%. Analytical data were in full agreement with those previously reported for the same compound [11]. Anal. Calc. for $C_{20}H_{24}O_3$: C 76.89, H 7.74, O 15.36; Found: C 76.81, H 7.71, O 15.36.

7-Farnesyloxy-4-methylcoumarin 25. Yellowish waxy solid. Yield 85%. Analytical data were in full agreement with those previously reported for the same compound [11]. Anal. Calc. for $C_{25}H_{32}O_3$: C 78.91, H 8.48, O 12.61; Found: C 78.88, H 8.53, O 12.67.

7-Isopentenyloxycoumarin-3-carboxylic acid 26. Yellow solid. Yield 81%. Analytical data were in full agreement with those previously reported for the same compound [3]. Anal. Calc. for $C_{15}H_{14}O_5$: C 65.69, H 5.15, O 29.17; Found: C 65.61, H 5.11, O 29.19.

2.3. Molecular modeling approaches

2.3.1. MetaCore/MetaDrug analysis

Metacore/MetaDrug is an integrated software package having

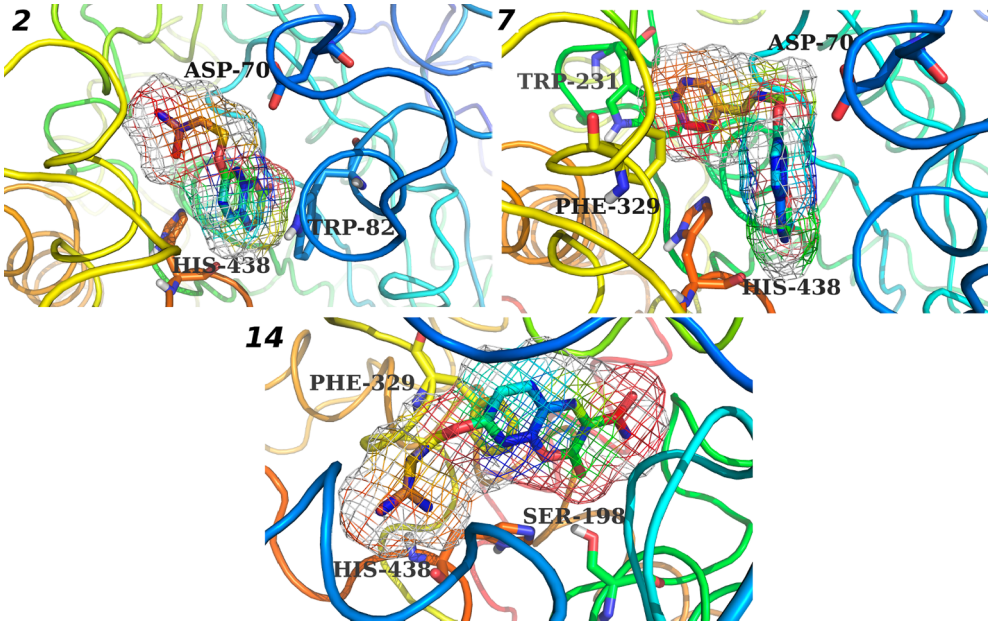

Fig. 4. 3D schematic views of the selected ligands inside the BChE target.

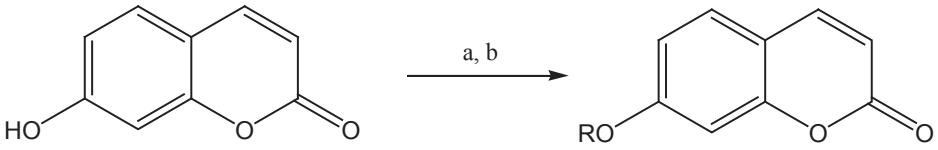

Scheme 1. Reagents and conditions: (a) alkyl bromide (1.0 equiv.), K_2CO_3 (1.5 equiv.), acetone, 80 °C, 1 h, (b) basic work-up.

manually curated biological information about small molecules. The MetaCore/MetaDrug platform of Clarivate analytics was used to predict therapeutic activity, toxicity and pharmacokinetic properties of used molecules. 26 different toxicity-QSAR models were used for the estimation of toxicity profiles of studied molecules such as cardiotoxicity, neurotoxicity, nephrotoxicity, mutagenicity, carcinogenicity, anemia, genotoxicity, cytotoxicity, kidney growth, hepatotoxicity, kidney necrosis, liver cholestasis, etc. The prediction of a therapeutic activity or toxic effect is calculated based on the ChemTree ability to correlate structural descriptors to that property using recursive partitioning algorithm. The ChemTree parameters that gave the best results were the following: path length 5, max segments 3, p-value threshold Bonnferoni 0.99, p-value multiway split 0.99 and number of the random trees 50. The training set used in MetaCore/MetaDrug includes molecules that possess the property (positives) and chemicals that do not have such property (negatives) in approximately equal numbers. The marketed drugs were used if their number was greater than 100 in the disease QSAR models, else drug candidates in clinical trials and preclinical compounds with in vivo activity have been added to the training set. The drugs that have been annotated to cause a particular toxic effect were used for the prediction of toxic effect. In order to choose the correct negative chemicals, the similarity of each negative chemical was calculated with respect to all positive chemicals and the highest value of similarity was recorded. Several ranges of negative drugs were generated for the training set starting from 0.9 similarity. Each similarity range stops at the value of similarity of a last drug that makes the amount of negatives equal to positives. The total of 6 ranges is generated from 0.9 to 0.4. In the end, one training set consists of all positives and the negatives from one similarity range. The training set is subjected to recursive partition analysis with default ChemTree parameters to select the best negative drugs for the model. The best training set from the previous step is used to generate 10 random training and test sets, so that the amount of molecules for the test set constitutes around 15–20% of the training set. The model is built based on the training set and is validated with the test set. The QSAR models used in MetaCore/MetaDrug is evaluated with specificity, sensitivity, accuracy, and Matthews Correlation Coefficient (MCC).

2.3.2. Protein preparation

The crystal structure of BChE was retrieved from the Protein Data Bank, (PDB entry: 4TPK) [12]. The missing atoms of the protein, such as hydrogen and side chains atoms were added and also the water molecules within the catalytic domain were kept using protein preparation wizard of Schrodinger suite [13]. The protein was assigned at a physiological pH by PROPKA code [14] and finally in order to refine the proteins, both side chains and backbone atoms were minimized with the forcefield method (OPLS2005) [15]. The ligand-binding cavity of the protein was determined based on the co-crystallized ligand position inside the crystal structure.

2.3.3. Molecular docking simulations

Docking protocols, including Glide XP (Extra Precision) [16] and ChemScore of GOLD [17] methods, were implemented to dock the potent compounds into the active site of the target. The binding energy values (docking scores) of the ligands inside the BChE were determined using the two docking protocols. The details of the methods used here were described in our previous work [18].

3. Results and discussion

3.1. Cholinesterase inhibition of the coumarin derivatives

A total of 26 coumarin compounds tested at 100 μM concentration displayed from none to weak inhibitory activity against AChE, whereas some of them exerted a noteworthy selective inhibition against BChE (Table 1). Besides, compounds **2**, **3**, **6**, **7**, **10–14**, and **23** possessed better IC_{50} values than that of the reference (galanthamine, IC_{50} = 46.58 ± 0.91 μM). The most active inhibitor was found to be compound **7** identified as 7-styryloxycoumarin.

Coumarins have been confirmed to exert a noticeable ChE inhibitory activity by many researchers. A recent report in agreement with our data indicated that 7-benzoyloxycoumarin exerted a marked inhibitory effect against BChE, which was also confirmed by experiments such as molecular energy, atomic charges, dipole moment, thermodynamic parameters, donor-acceptor natural bond orbital (NBO) hyperconjugative interaction energies, frontier molecular orbitals energies, HOMO-LUMO gap, molecular electrostatic potential, chemical reactivity descriptors, molecular polarizability and non-linear optical (NLO) properties [11]. Besides Kapp et al. proposed that substitution at either 4th or 7th position could lead a selective inhibition towards cholinesterases, which is also consonant to our present data [19]. Among the coumarin derivatives screened herein, umbelliprenin (the umbelliferone having a farnesyloxy side chain) was found to possess no inhibition against AChE as well as low inhibitory effect (26.66 ± 1.11%) against BChE, whereas 6-formyl-umbelliferone was reported to inhibit them modestly [20]. This might be commented as prenylation may lower ChE inhibitory activity. In the same study, molecular docking experiments pointed out to interaction of 6-formyl-umbelliferone with both the catalytic active sites and peripheral anionic sites of AChE, while our compounds with the highest inhibitory activity (**2**, **7**, and **14**) interacted with only the catalytic active site of BChE. Ali et al. also suggested that presence or absence of an aldehyde group at the C-8 position reduced anticholinesterase activity [20].

In a series of 7-substituted coumarin derivatives synthesized recently by Joubert et al. [21], two of them were revealed to be multifunctional lead molecules as selective BChE inhibitors, which is again consistent with our current findings. On the other hand, 3-chloro-substitution on coumarin derivatives seems to cause inactivation against cholinesterases according to our results (Table 1). A similar trend has been already observed in the case of unprenylated 3-chloro-substituted coumarins, *e.g.* 3-chloro-7-hydroxy-4-methylcoumarin, the parent compound of samples **17–19**, as reported in 1991 by Radic and co-workers [22]. In general, in fact it has been already pointed out the importance of leaving untouched position 3 respect to the original coumarin skeleton (*e.g.* presence of only hydrogen atoms) for the observed inhibitory activity on cholinesterases [23].

3.2. MetaCore/MetaDrug analysis

Table 2 shows pharmacokinetic profiles of the studied compounds. According to the results obtained, all compounds have lipophilic character and permeate blood brain barrier (BBB). ADME models predict higher human serum protein binding percentages (> 50%) for all compounds. A model based on retention times of compounds assayed by HPLC using an immobilized human serum albumin (HAS) column was used and it is found that retention time of all compounds were low.

Results were also clear that the compounds do not have a high binding affinity for hERG (human ether a-go-go-related gene) channel inhibition as well as human serotonin transporter inhibition. While Table S1 shows therapeutic activity prediction, Table 3 shows toxicity prediction values for the studied molecules. The lowest toxicity prediction was found for the compound **24**, where this compound showed higher values than threshold in only 4 toxicity models. Epididymis toxicity and liver cholestasis were found high for all compounds in these models.

3.3. Molecular docking simulations

The compounds which are revealing inhibitory activities against BChE target were used into molecular docking simulations. The binding energies of the ligands at the binding pocket of the target were estimated using both Glide/XP and GOLD/ChemScore protocols, as shown in Fig. 2. The binding energy values, obtained by the GOLD method, are roughly lower in comparison with those calculated by the Glide/XP method – this can be due to the parameters and factors implemented to score the energy values. Interestingly, the binding energy of compound **7** was determined to be −8.91 kcal/mol by GOLD ChemScore, which is consistent with the *in vitro* data as the best BChE inhibitor among other studied ligands. However, the docking scores calculated by both methods revealed that all the active compounds have favorable free binding energies in interacting with the ligand-binding domain of the target.

In order to study, the inhibition mechanisms of the ligands inside the catalytic domain of BChE, the three best active compounds, namely **2**, **7**, and **14**, were selected to investigate their chemical interactions established with the active site amino acids. The positions of the ligands and the important polar and nonpolar contacts between the ligands and the amino acids were shown in both 2D and 3D schematic views (Figs. 3 and 4). Compound **2** established strong two π-π stacking interactions from its aromatic rings with Trp82, and also a water-mediated hydrogen bond interaction between the polar site of the ligand and Gly197. Compound **7**, which was found as the best inhibitor, in addition to the hydrogen bond formed by Gly197, stacked with Trp231 and Phe329 within the binding domain. It seems that compound **14** revealed a different conformation in comparison with the others, forming π-π stacking interactions with Phe329, as shown in Fig. 2. The results demonstrated that the selected ligands were able to be accommodated well inside the binding domain of BChE by the polar and nonpolar amino acids.

4. Conclusion

In the current study, 26 O-alkylcoumarin derivatives were tested for their cholinesterase inhibitory activity and 12 of them displayed a noteworthy inhibition towards BChE. Among them, the best inhibitory compound was revealed to be 7-styryloxycoumarin (IC_{50} = 7.01 ± 0.28 μM) by both *in vitro* screening and *in silico* experiments. Structure-activity relationship considerations led to hypothesize that introduction of lipophilic moieties as substituents alternative to free OH groups represents an effective means to increase the inhibitory activities on ChE. This kind of structural substitution has first a deep influence on the pharmacokinetic properties of herein synthesized coumarins in respect to native OH free compounds. Pharmacokinetic data in fact showed that all compounds have lipophilic character and permeate blood brain barrier (BBB). This may have a great potential considering that putative ChE inhibitors may be used as pharmacologically active agents against severe neurological disorders. The binding energy values calculated using docking simulations are favorable and suggested that strong polar and nonpolar interactions were formed between the ligand atoms and the active site amino acids of BChE. Thus, a second important acquisition from our studies is that the presence of large, bulky, and conformationally rigid moieties provide substituted coumarins having a greater selectivity towards BChE. Such a result may arise from a tight interaction of the styryl moiety with a specific aminoacidic portion of the active site of BChE.

Conflicts of interest

The authors declare no competing financial interest.

Appendix A. Supplementary material

Supplementary data to this article can be found online at https://doi.org/10.1016/j.bioorg.2018.11.044.

References

[1] A. Vogel, Darstellung von Benzoesäure aus der Tonka-Bohne und aus den Meliloten - oder Steinklee - Blumen, Ann. der Phys. und der Phys. Chemie 64 (1820) 161–166.
[2] K.M. Venkata Sairam, B.S. Gurupadayya, R.K. Chandan, D. Nagesha, B. Vishwanathan, A review on chemical profile of coumarins and their therapeutic role in the treatment of cancer, Curr. Drug Deliv. 13 (2016) 186–201.
[3] M. Curini, G. Cravotto, F. Epifano, G. Giannone, Chemistry and biological activity of natural and synthetic prenyloxycoumarins †, Curr. Med. Chem. 13 (2006) 199–222.
[4] I.E. Orhan, H.O. Gulcan, Coumarins: auspicious cholinesterase and monoamine oxidase inhibitors, Curr. Top. Med. Chem. 15 (2015) 1673–1682.
[5] K. Skalicka-Woźniak, I.E. Orhan, G.A. Cordell, S.M. Nabavi, B. Budzyńska, Implication of coumarins towards central nervous system disorders, Pharmacol. Res. 103 (2016) 188–203.
[6] L.G. De Souza, M.N. Rennó, J.D. Figueroa-Villar, Coumarins as cholinesterase inhibitors: A review, Chem. Biol. Interact. 254 (2016) 11–23.
[7] G.L. Delogu, M.J. Matos, Coumarins as promising scaffold for the treatment of age-related diseases - an overview of the last five years, Curr. Top. Med. Chem. 17 (29) (2017) 3173–3189.
[8] M. Gargaro, F. Epifano, S. Fiorito, V.A. Taddeo, S. Genovese, M. Pirro, A. Turco, P. Puccetti, C.B. Schmidt-Weber, F. Fallarino, Interaction of 7-alkoxycoumarins with the aryl hydrocarbon receptor, J. Nat. Prod. 80 (2017) 1939–1943.
[9] G.L. Ellman, K.D. Courtney, V. Andres, R.M. Featherstone, A new and rapid colorimetric determination of acetylcholinesterase activity, Biochem. Pharmacol. 7 (1961) 88–95.
[10] I.E. Orhan, D. Jedrejek, F.S. Senol, R.E. Salmas, S. Durdagi, I. Kowalska, L. Pecio, W. Oleszek, Molecular modeling and in vitro approaches towards cholinesterase inhibitory effect of some natural xanthohumol, naringenin, and acyl phloroglucinol derivatives, Phytomedicine 42 (2018) 25–33.
[11] M. Alam, M.J. Alam, S. Azaz, M. Parveen, S. Park, S. Ahmad, DFT/TD-DFT calculations, spectroscopic characterizations (FTIR, NMR, UV–vis), molecular docking and enzyme inhibition study of 7-benzoyloxycoumarin, Comput. Biol. Chem. 73 (2018) 65–78.
[12] B. Brus, U. Košak, S. Turk, A. Pišlar, N. Coquelle, J. Kos, J. Stojan, J.-P. Colletier, S. Gobec, Discovery, biological evaluation, and crystal structure of a novel nanomolar selective butyrylcholinesterase inhibitor, J. Med. Chem. 57 (2014) 8167–8179.
[13] G. Madhavi Sastry, M. Adzhigirey, T. Day, R. Annabhimoju, W. Sherman, Protein and ligand preparation: parameters, protocols, and influence on virtual screening enrichments, J. Comput. Aided. Mol. Des. 27 (2013) 221–234.
[14] D.C. Bas, D.M. Rogers, J.H. Jensen, Very fast prediction and rationalization of pKa values for protein-ligand complexes, Proteins Struct. Funct. Bioinforma. 73 (2008) 765–783.
[15] J.L. Banks, H.S. Beard, Y. Cao, A.E. Cho, W. Damm, R. Farid, A.K. Felts, T.A. Halgren, D.T. Mainz, J.R. Maple, R. Murphy, D.M. Philipp, M.P. Repasky, L.Y. Zhang, B.J. Berne, R.A. Friesner, E. Gallicchio, R.M. Levy, Integrated modeling program, applied chemical theory (IMPACT), J. Comput. Chem. 26 (2005) 1752–1780.
[16] T.A. Halgren, R.B. Murphy, R.A. Friesner, H.S. Beard, L.L. Frye, W.T. Pollard, J.L. Banks, Glide: a new approach for rapid, accurate docking and scoring. 2. Enrichment factors in database screening, J. Med. Chem. 47 (2004) 1750–1759.
[17] M.L. Verdonk, J.C. Cole, M.J. Hartshorn, C.W. Murray, R.D. Taylor, Improved protein-ligand docking using GOLD, Proteins Struct. Funct. Bioinforma. 52 (2003) 609–623.
[18] R.E. Salmas, P. Seeman, B. Aksoydan, I. Erol, I. Kantarcioglu, M. Stein, M. Yurtsever, S. Durdagi, Analysis of the glutamate agonist LY404,039 binding to nonstatic dopamine receptor d2 dimer structures and consensus docking, ACS Chem. Neurosci. 8 (2017) 1404–1415.
[19] E. Kapp, H. Visser, S. Sampson, S. Malan, E. Streicher, G. Foka, D. Warner, S. Omoruyi, A. Enogieru, O. Ekpo, F. Zindo, J. Joubert, Versatility of 7-substituted coumarin molecules as antimycobacterial agents, neuronal enzyme inhibitors and neuroprotective agents, Molecules 22 (2017) 1644.
[20] M.Y. Ali, S.H. Seong, M.R. Reddy, S.Y. Seo, J.S. Choi, H.A. Jung, Kinetics and molecular docking studies of 6-formyl umbelliferone isolated from angelica decursiva as an inhibitor of cholinesterase and BACE1, Molecules (2017).
[21] J. Joubert, G.B. Foka, B.P. Repsold, D.W. Oliver, E. Kapp, S.F. Malan, Synthesis and evaluation of 7-substituted coumarin derivatives as multimodal monoamine oxidase-B and cholinesterase inhibitors for the treatment of Alzheimer's disease, Eur. J. Med. Chem. 125 (2017) 853–864.
[22] Z. Radić, E. Reiner, P. Taylor, Role of the peripheral anionic site on acetylcholinesterase: inhibition by substrates and coumarin derivatives, Mol. Pharmacol. 39 (1991) 98–104.
[23] P. Anand, B. Singh, N. Singh, A review on coumarins as acetylcholinesterase inhibitors for Alzheimer's disease, Bioorg. Med. Chem. 20 (2012) 1175–1180.